



At High Levels, Constitutively Activated STAT3 Induces Apoptosis of Chronic Lymphocytic Leukemia Cells

This information is current as
of February 26, 2022.

Uri Rozovski, David M. Harris, Ping Li, Zhiming Liu, Ji
Yuan Wu, Srdana Grgurevic, Stefan Faderl, Alessandra
Ferrajoli, William G. Wierda, Matthew Martinez, Srdan
Verstovsek, Michael J. Keating and Zeev Estrov

J Immunol 2016; 196:4400-4409; Prepublished online 13
April 2016;
doi: 10.4049/jimmunol.1402108
<http://www.jimmunol.org/content/196/10/4400>

**Supplementary
Material** <http://www.jimmunol.org/content/suppl/2016/04/13/jimmunol.1402108.DCSupplemental>

References This article **cites 46 articles**, 21 of which you can access for free at:
<http://www.jimmunol.org/content/196/10/4400.full#ref-list-1>

Why *The JI*? [Submit online.](#)

- **Rapid Reviews! 30 days*** from submission to initial decision
- **No Triage!** Every submission reviewed by practicing scientists
- **Fast Publication!** 4 weeks from acceptance to publication

**average*

Subscription Information about subscribing to *The Journal of Immunology* is online at:
<http://jimmunol.org/subscription>

Permissions Submit copyright permission requests at:
<http://www.aai.org/About/Publications/JI/copyright.html>

Email Alerts Receive free email-alerts when new articles cite this article. Sign up at:
<http://jimmunol.org/alerts>

At High Levels, Constitutively Activated STAT3 Induces Apoptosis of Chronic Lymphocytic Leukemia Cells

Uri Rozovski, David M. Harris, Ping Li, Zhiming Liu, Ji Yuan Wu, Srdana Grgurevic, Stefan Faderl, Alessandra Ferrajoli, William G. Wierda, Matthew Martinez, Srdan Verstovsek, Michael J. Keating, and Zeev Estrov

In chronic lymphocytic leukemia (CLL), the increment in PBLs is slower than the expected increment calculated from the cells' proliferation rate, suggesting that cellular proliferation and apoptosis are concurrent. Exploring this phenomenon, we found overexpression of caspase-3, higher cleaved poly (ADP-ribose) polymerase levels ($p < 0.007$), and a higher apoptosis rate in cells from patients with high counts compared with cells from patients with low counts. Although we previously found that STAT3 protects CLL cells from apoptosis, STAT3 levels were significantly higher in cells from patients with high counts than in cells from patients with low counts. Furthermore, overexpression of STAT3 did not protect the cells. Rather, it upregulated *caspase-3* and induced apoptosis. Remarkably, putative STAT3 binding sites were identified in the *caspase-3* promoter, and a luciferase assay, chromatin immunoprecipitation, and an EMSA revealed that STAT3 activated *caspase-3*. However, caspase-3 levels increased only when STAT3 levels were sufficiently high. Using chromatin immunoprecipitation and EMSA, we found that STAT3 binds with low affinity to the *caspase-3* promoter, suggesting that at high levels, STAT3 activates proapoptotic mechanisms and induces apoptosis in CLL cells. *The Journal of Immunology*, 2016, 196: 4400–4409.

Chronic lymphocytic leukemia (CLL) is characterized by a gradual accumulation of monoclonal, dysfunctional mature-appearing lymphocytes (1). Traditionally, CLL cells were thought to have a prolonged lifespan because of a deregulated apoptosis pathway (2–4). Studies performed during the past decade revealed that CLL cells proliferate and undergo spontaneous apoptosis. Ki-67, typically expressed in proliferating cells, was found in an appreciable number of CLL bone marrow cells, and TUNEL also revealed apoptosis in CLL bone marrow cells (5). Deuterated water studies showed that 0.1–1.75% of the CLL clone is regenerated daily (6). However, the increment in peripheral blood (PB) CLL cell counts is typically lower than is expected from the cells' proliferation rate. Therefore, it was assumed that CLL cell proliferation is accompanied by spontaneous apoptosis.

STAT3 is a latent cytoplasmic transcription factor that upon phosphorylation and dimerization shuttles to the nucleus, binds to DNA (7), and activates STAT3-regulated genes. In various solid tumors and hematologic malignancies, including CLL, STAT3 is constitutively activated and provides neoplastic cells with proliferation signals and a survival advantage (8–17).

Because in CLL cells, STAT3 is constitutively phosphorylated on serine 727 residues and activates antiapoptotic genes (10, 12–14), we hypothesized that high STAT3 levels inversely correlate with the apoptosis rate in CLL cells. Surprisingly, we found that when STAT3 levels were sufficiently high, STAT3 no longer protected CLL cells from apoptosis. Instead, STAT3 induced the expression of proapoptotic genes, activated the caspase-3 gene promoter, and induced apoptosis in CLL cells.

Materials and Methods

Patient characteristics

PB samples were obtained from 64 patients with CLL who were treated at The University of Texas MD Anderson Cancer Center Leukemia Clinic between April 2008 and May 2011, after approval was obtained from the Institutional Review Board, and written informed consent was obtained from the patients. PB counts of 320 consecutive patients with CLL were evaluated to determine the means \pm SD of lymphocyte counts in the 10% of patients with the highest counts ($n = 32$; mean $140,000 \pm 49,738 \times 10^9/l$) and the 10% of patients with the lowest counts ($n = 32$; mean $12,800 \pm 4,564 \times 10^9/l$). Of the 64 patients, 54 (84%) had not received any prior treatment for CLL. The remaining 10 previously treated patients were evenly distributed between the subgroups of patients with a high or low lymphocyte count. The clinical characteristics of all the patients are depicted in Supplemental Table I.

Cell fractionation

PB cells were fractionated using Ficoll Hypaque 1077 (Sigma-Aldrich, St. Louis, MO). The low-density cellular fraction was used immediately or frozen for additional studies.

Western Immunoblotting

Western immunoblotting was performed as previously described (18). Briefly, CLL cell extract was prepared. The protein concentration was

Department of Leukemia, The University of Texas MD Anderson Cancer Center, Houston, TX 77030

ORCID: 0000-0002-0195-0871 (P.L.).

Received for publication August 15, 2014. Accepted for publication March 10, 2016.

This work was supported by a grant from the CLL Global Research Foundation. The University of Texas MD Anderson Cancer Center is supported in part by the National Institutes of Health through a Cancer Center Support Grant (P30CA16672).

U.R., M.J.K., and Z.E. were responsible for conception and design; U.R. was responsible for statistical and bioinformatics analysis; S.F., A.F., W.G.W., S.V., M.J.K., and Z.E. were responsible for provision of study materials or patients; J.Y.W. was responsible for collection and assembly of data; D.M.H. performed the propidium iodide/Annexin assay; P.L. performed quantitative RT-PCR EMSA and chromatin immunoprecipitation experiments; D.M.H., Z.L., S.G., and M.M. performed the ELISA experiments; U.R. and Z.E. were responsible for manuscript writing; and final approval of manuscript was done by all authors.

Address correspondence and reprint requests to Dr. Zeev Estrov, Department of Leukemia, The University of Texas MD Anderson Cancer Center, Unit 428, 1515 Holcombe Boulevard, Houston, TX 77030. E-mail address: zestrov@mdanderson.org

The online version of this article contains supplemental material.

Abbreviations used in this article: ChIP, chromatin immunoprecipitation; CLL, chronic lymphocytic leukemia; GAS, γ -IFN activation sequence; PARP, poly (ADP-ribose) polymerase; PB, peripheral blood; PI, propidium iodide; qRT-PCR, quantitative RT-PCR.

Copyright © 2016 by The American Association of Immunologists, Inc. 0022-1767/16/\$30.00

determined using a Micro BCA protein assay reagent kit (Thermo Scientific, Pierce, Rockford, IL). Cell lysates were denatured and, following electrophoresis, transferred to a nitrocellulose membranes. The membranes were incubated with monoclonal mouse anti-human STAT3 (BD Biosciences, Palo Alto, CA), polyclonal rabbit anti-human phosphoserine (serine 727) STAT3 (Cell Signaling Technology, Beverly, MA), caspase-3 (Cell Signaling Technology), cleaved caspase-3 (BD Biosciences), monoclonal STAT1 (BD Biosciences), phosphoserine STAT1 (serine 727) (BD Biosciences), or monoclonal mouse anti-human β -actin (Sigma-Aldrich) HRP-conjugated secondary Abs (GE Healthcare, Amersham, Buckinghamshire, U.K.). Proteins were visualized via an ECL detection system (GE Healthcare).

Densitometry analysis was performed using an Epson Expression 1680 scanner (Epson America, Long Beach, CA). Densitometry values were normalized by dividing the numerical value of each sample signal by the numerical value of the signal from the corresponding actin protein levels used as loading control.

Annexin V/propidium iodide assay

The rate of cellular apoptosis was analyzed using double staining with a Cy5-conjugated Annexin V kit and propidium iodide (PI; BD Biosciences) according to the manufacturer's instructions. After incubation for 10 min in the dark at room temperature, the samples were analyzed on an FACS-Calibur flow cytometer (BD Biosciences). Cell viability was calculated as the percentage of Annexin V-positive cells.

RNA extraction

After thawing in hot water, cells were washed twice with RPMI 1640 (Life Technologies), and TRIzol (Invitrogen, Carlsbad, CA) was added. The RNA was isolated using an RNeasy purification kit (Qiagen, Valencia, CA). RNA quality and concentration were analyzed with a NanoDrop spectrophotometer (ND-1000; NanoDrop Technologies, Wilmington, DE).

Quantitative RT-PCR analysis

We used 500 ng total RNA in one-step quantitative RT-PCR (qRT-PCR; Applied Biosystems, Foster City, CA) analysis with an ABI Prism 7700 sequence detection system (Applied Biosystems) using a TaqMan gene expression assay for MAPK 8, KRAS, phospholipase C γ 2, p-ERK, calpain9, and caspase-3 according to the manufacturer's instructions. Samples were run in triplicate, and relative quantification was performed by using the comparative threshold cycle method (13).

Microarray analysis

Hybridization was performed with Human Gene 2.0 ST arrays (Affymetrix, Santa Clara, CA) according to the manufacturer's instructions. Briefly, 100 ng total RNA from each sample was reverse transcribed to cDNA, followed by overnight in vitro transcription to generate cRNA, which was also reverse transcribed. The quality of cDNA and fragmented cDNA was assessed using an Agilent Bioanalyzer system. Microarrays were hybridized, washed, and stained, and images were scanned using the Affymetrix GeneChip Command Console and analyzed with the Affymetrix Expression Console. The *t* test with Welch correction (variance not assumed equal) was used to compare gene expression levels, and the analysis was done using Partek Genomics Suite 6.6 (Partek, St. Louis, MO). Network analysis was performed on 1001 genes for which levels were upregulated ($p < 0.01$ in samples with at least a 1.5-fold increase in lymphocyte counts) using the Ingenuity pathway analysis (Ingenuity Systems, www.ingenuity.com). The data are provided at <http://www.ncbi.nlm.nih.gov/geo/query/acc.cgi?acc=GSE68721>.

ELISA

Levels of cleaved poly (ADP-ribose) polymerase (PARP) were determined using an Invitrogen Cleaved PARP ELISA kit (Invitrogen) according to the manufacturer's instructions. Briefly, microtiter wells were coated with mouse anti-rabbit uncleaved (116 kD) or cleaved (85 kD) PARP Abs. Cleaved PARP levels were assessed by comparing the color intensity of the tested samples with that of the standard cleaved PARP protein levels provided in the kit using a microplate autoreader (Model #EL309; Bio-Tek Instruments, Winooski, VT).

Transfection of MM-1 cells with the human STAT3 gene

The human STAT3 sequence was obtained from GenBank NM_139276, and its full-length coding sequence was generated via PCR from the human STAT3 cDNA clone (OriGene, SC124165). The primers used for generation of rSTAT3 were: STAT3-Full, 5'-GCGGCGCGGCCGCCGCCGCCAC-CATGGCCCAATGGAATCAGCTACAG-3' and STAT3, 3'-GCGGCGCTCG-AGTAACATGGGGGAGGTAGCGCAC-5'. The sense primer contained a NotI

site, a Kozac codon, and a gene-specific sequence (starting from ATG), and the antisense primers contained an XhoI site and a coding sequence ending at 2313 bp with a mutant stop codon. The PCR products were digested with NotI and XhoI and subcloned into the mammalian expression vector pBudCE4.1 (Invitrogen). GFP was cloned into another cloning site with HindIII/XbaI. MM-1 cells were transfected via electroporation with a Gene Pulser Xcell electroporation system (Bio-Rad, Hercules, CA) set at 120 mV with one pulse. Transfection efficiency was detected using fluorescence microscopy and flow cytometry. After the transfection, cells were incubated for 24 or 48 h with 50 ng/ml recombinant human IL-6 (Life Technologies, Frederick, MD) and harvested for qRT-PCR analysis.

Infection of CLL cells with the human STAT3

Full-length human STAT3 was amplified from the human STAT3 cDNA clone (SC124165; OriGene, Rockville, MD), cloned using SalI/EcoRV into pENTR11 (Invitrogen), and sequence-verified. Both GFP and STAT3 were transferred into pInducer20 (plasmid 44012; Addgene, Cambridge, MA), and after overnight infection, protein expression was induced using 1 μ g/ml doxycycline (Sigma-Aldrich). The lentiviral vector was produced by transfecting the plasmid into HEK293T cells using the Lipofectamine 2000 transfection reagent (Invitrogen). pINDUCER20 STAT3 and the GFP expression vectors were transfected with the packaging vectors pMDLg/pRRE, pRSV-Rev, and pMD2.G (Addgene). HEK293T cells were expanded in culture, and their supernatant was used to infect the CLL cells as previously described (10).

Transfection of MM-1 cells with caspase-3 promoter fragments and luciferase assay

Caspase-3 promoter fragments were transfected into MM-1 cells via electroporation as described above. Each construct included a luciferase reporter gene 770 bp upstream to the transcription starting site of the caspase-3 gene that did not include γ -IFN activation sequence (GAS)-like elements or 854 bp upstream to the caspase-3 gene transcription starting site that included a single GAS-like element. The luciferase activity of unstimulated or IL-6-stimulated MM-1 cells was assessed 24 h after transfection using a Dual-Luciferase Reporter Assay System (Promega) and a Sirius luminometer V3.1 (Berthold Detection Systems, Pforzheim, Germany). The luciferase activity of each of the human caspase-3 promoter constructs was determined by calculating the constructs' luciferase activity relative to the activity of the Renilla luciferase produced by the PGL4-17 control vector.

Chromatin immunoprecipitation assay

A chromatin immunoprecipitation (ChIP) assay was performed using a SimpleChIP Enzymatic Chromatin IP Kit (Cell Signaling Technology, Boston, MA) according to the manufacturer's instructions. Briefly, cells were cross-linked with 1% formaldehyde for 10 min at room temperature and then harvested and incubated on ice for 10 min in lysis buffer. Nuclei were pelleted and digested with micrococcal nuclease. Following sonication and centrifugation, sheared chromatin was incubated with anti-STAT3 or rabbit serum (negative control) overnight at 4°C. Then, protein G beads were added, and the chromatin was incubated for 2 h in rotation. Ab-bound protein-DNA complexes were eluted and subjected to PCR analysis. The primer sets used to amplify the caspase-3 promoter putative STAT3 binding sites were as follows: set 1, 5'-914TCCCAACAGCCGGCTTAA-3' and 3'-849AAGAAGCCTGGTTTGGC-5'; set 2, 5'-1172CAGACC-CAAAATAGGAA-3' and 3'-1047GCTTGTGGCAAATGCCT-5'; set 3, 5'-1299GTCCCTGAATCTGACTTC-3' and 3'-1177CATTTTCAGA-CCCTGAAGC-5'; and set 4, 5'-1706GTAGCTGGGATTACAGGT-3' and 3'-1625CAAGATGGTGAAACCCTG-5'.

EMSA

Nondenatured cellular nuclear extracts were prepared using a NE-PER extraction kit (Thermo Scientific Pierce, Rockford, IL). Nuclear protein extracts were incubated with biotin-labeled caspase-3, c-myc, and STAT3 promoters' DNA probes in binding buffer for 30 min on ice. All probes were synthesized by Sigma-Genosys (The Woodlands, TX). Following incubation, the samples were separated on a 5% polyacrylamide gel, transferred onto a nylon membrane, and fixed on the membrane via UV cross-linking. The biotin-labeled probe was detected with streptavidin-HRP (Gel-Shift Kit; Panomics, Fremont, CA). The control consisted of 7-fold excess unlabeled cold probe. To test the effect of STAT3, anti-STAT3 Abs (BD Biosciences) or mouse IgG1 (BD Biosciences) were added with the nuclear extracts (10, 19).

Results

High lymphocyte counts are correlated with high levels of STAT3

Because in CLL STAT3 is constitutively phosphorylated on serine 727 residues (10), and because STAT3 promotes the proliferation and survival of cancer cells, including CLL cells (20, 21), we assumed that CLL cells from patients with a high tumor burden would harbor high levels of STAT3. To test this hypothesis, we obtained PB cells from patients with a low ($n = 32$) and high ($n = 32$) lymphocyte count. Compared with patients with low lymphocyte counts (mean: $12,800 \pm 4,654 \times 10^9/l$), patients with high counts (mean: $145,000 \pm 49,738 \times 10^9/l$) had advanced disease, high levels of β_2 -microglobulin levels, and unmutated IgH gene status (Supplemental Table 1). Western blot analysis revealed that CLL cells from patients with a high lymphocyte count harbored higher levels of total STAT3 compared with patients with low counts ($p = 0.03$), whereas overall the levels of serine p-STAT3 were similar in patients with high and low counts as assessed by densitometry (Fig. 1A). High lymphocyte counts correlated with high levels of STAT3 ($r_s = 0.5$; $p < 0.0001$) (Fig. 1B). Because STAT1 is constitutively phosphorylated on serine 727 residues (22) and induces apoptosis in CLL cells (23), we assessed the levels of STAT1 and pSTAT1 in patients with high ($n = 4$) and low ($n = 4$) lymphocyte counts. Contrary to STAT3, levels of STAT1 and serine p-STAT1 were similar in patients with high and low lymphocyte counts (Fig. 1C).

High lymphocyte counts are correlated with high rates of spontaneous apoptosis

Previous studies showed that ~1% of the entire CLL clone divides daily (24). Because the actual increase in the PB lymphocyte count is lower than the expected lymphocyte count estimated using the CLL cell proliferation rate, we hypothesized that CLL cell proliferation is associated with concomitant spontaneous apoptosis. Using Annexin V and PI staining, we assessed the spontaneous apoptosis rate of fresh PB low-density cells obtained from patients with CLL and found that CLL cell apoptosis rates correlated with WBC counts ($r_p = 0.88$; $p = <0.0001$) (Fig. 2A). For example, the spontaneous apoptosis rate of CLL PB low-density cells (>98% lymphocytes) from a patient with a WBC count of $16 \times 10^9/l$ was 23%, whereas the spontaneous apoptosis rate of CLL PB cells from a patient with a WBC count of $101 \times 10^9/l$ was 65% (Fig. 2B). Because similar experiments (data not shown) revealed a similar trend, we sought to determine whether high lymphocyte counts correlated with a high apoptosis rate.

To test our hypothesis, we first analyzed the gene signature profile of CLL cells from 9 patients with high ($n = 4$) and low ($n = 5$) lymphocyte counts. The same trend in gene expression was validated by qRT-PCR, and pathway analysis revealed that the apoptosis signaling pathway was enriched with genes for which levels were high in CLL cells from patients with high lymphocyte counts ($p = 0.02$). Specifically, *caspase-3*, *MAPK 8*, *KRAS*, *phospholipase C γ 2*, *protein kinase C*, *calpain 9*, and *caspase-3* were incorporated in this pathway (Supplemental Fig. 1).

Taken together, these results suggest that the apoptosis signaling pathway is activated in CLL cells from patients with high lymphocyte counts and that those cells undergo spontaneous apoptosis at a high rate. To further delineate these findings, we obtained cells from patients with CLL with high ($n = 16$) and low ($n = 16$) lymphocyte counts and, using ELISA, assessed the levels of cleaved PARP. PARP, known to protect cellular integrity, is cleaved and inactivated by cleaved caspase-3. We found that the median level of cleaved PARP was significantly higher in cells from patients with high lymphocyte counts (median 0.03; range 0.02–0.07) than in cells from patients with low lymphocyte counts (median 0.06; range 0.03–0.46), ($p < 0.007$) (Fig. 3).

Overexpression of STAT3 upregulates caspase-3 levels and induces apoptosis

Although STAT3 is a transcription factor that provides CLL cells with a survival advantage, and its levels are high in lymphocytes from patients with CLL with high lymphocyte counts (Fig. 1), CLL cells from patients with high lymphocyte counts undergo spontaneous apoptosis at a higher rate than cells obtained from patients with low lymphocyte counts who harbor lower STAT3 levels (Figs. 2, 3). To determine whether high levels of STAT3 induce apoptosis, we transfected MM-1 cells with a vector containing the rSTAT3 DNA construct and used Annexin/PI staining to assess the cellular apoptosis rate. As shown in Fig. 4A, 85% of cells transfected with STAT3 underwent apoptosis, as opposed to 59% of cells that were transfected with the empty vector (44% difference).

Because the protein levels of caspase-3, an essential proapoptotic protein activated downstream of both the intrinsic and extrinsic apoptotic pathways, were significantly increased in CLL cells from patients with a high lymphocyte count, and overexpression of STAT3 in MM-1 cells induced apoptosis (Fig. 4A), we sought to determine whether there is a cause-and-effect association between STAT3 and caspase-3. Therefore, we transfected MM-1 cells with rSTAT3 DNA and using qRT-PCR assessed STAT3 and caspase-3 RNA levels 24 h after the transfection. Transfection of MM-1 cells with *STAT3* induced a 7.5-fold increase in *STAT3* expression levels and a 2.5-fold increase in *caspase-3* expression levels (Fig. 4B). Similarly, infection of CLL cells with a lentivirus harboring the full-length human *STAT3* induced an increase in *STAT3* and *caspase-3* expression, an increase in STAT3 and cleaved caspase-3 protein levels (Fig. 4C), and an increase in apoptosis rate of CLL cells (Fig. 4D).

STAT3 binds and activates the promoter of the caspase-3 gene

Because overexpression of STAT3 resulted in increased caspase-3 RNA levels, we sought to determine whether STAT3 directly activates the caspase-3 gene. We conducted a sequence analysis of the caspase-3 gene promoter and identified within the promoter six GAS-like elements thought to be STAT3 binding sites (Fig. 5A, *top panel*). Then, to determine whether STAT3 activates the *caspase-3* promoter, we transfected MM-1 cells with the luciferase reporter gene driven by truncated fragments of the *caspase-3* promoter. Because in unstimulated MM-1 cells STAT3 is not activated (25), we incubated the cells with IL-6 that induces phosphorylation of STAT3 on tyrosine 705 residues (10, 26, 27). IL-6-induced luciferase activity was detected in the 854-bp fragment that harbors putative STAT3 binding sites but not in shorter fragments lacking those sites (Fig. 5A, *bottom panel*). Then, using ChIP, we found that DNA fragments detected by primers 1, 2, and 4, but not primer 3, each corresponding to a single GAS-like element (Fig. 5A), coimmunoprecipitated with STAT3 (Fig. 5B), suggesting that STAT3 binds to sites 1, 2, and 4 (but not site 3) of the *caspase-3* promoter. To confirm that STAT3 binds to the caspase-3 gene promoter, we performed EMSA using a biotinylated DNA probe of binding site 1 of the caspase-3 promoter. MM-1 nuclear protein extract bound to and formed a complex with the caspase-3 DNA promoter, and the binding was completely reversed by the addition of excess unlabeled probe or attenuated by anti-STAT3 Abs, whereas no binding was detected when a biotinylated mutated site 1 DNA probe was used (Fig. 5C).

STAT3 binds with low affinity to the caspase-3 gene promoter of CLL cells

To validate that STAT3 binds to the caspase-3 gene promoter in CLL cells as well, we incubated nuclear extracts of PB CLL cells from two patients with high lymphocyte counts with the biotinylated DNA probe of binding site 1 as described in the previous section. CLL cell nuclear extracts bound to and formed complexes

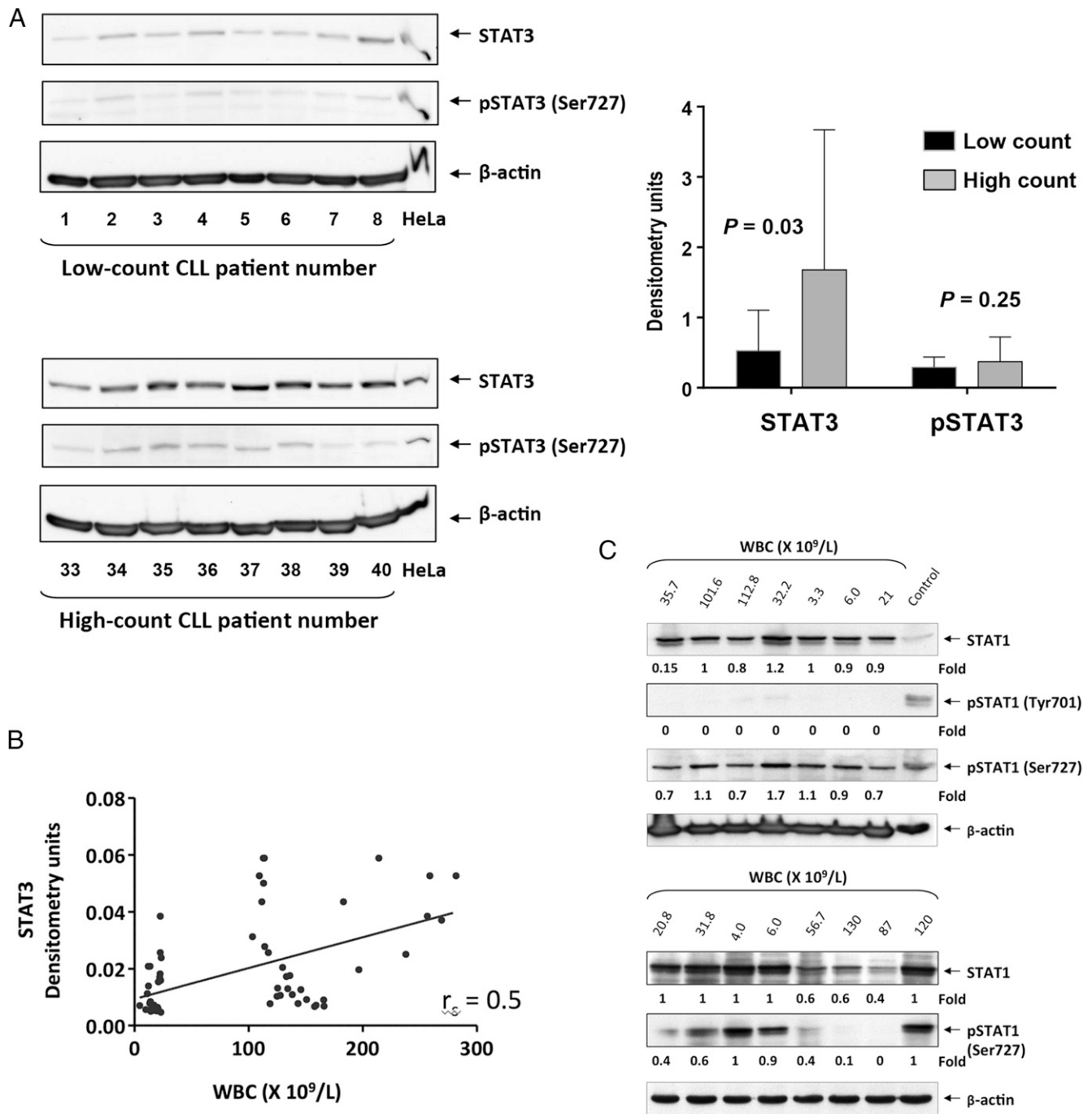


FIGURE 1. STAT3 levels are higher and STAT1 levels are lower in high-count compared with low-count CLLs. **(A)** Left panel, Western immunoblot of CLL cells from patients with low and high lymphocyte counts. The figure depicts blots of eight patients with low lymphocyte counts (top panel) and eight patients with high lymphocyte counts (bottom panel). Anti-STAT3 and anti-serine p-STAT3 Abs were used. Actin was used as the loading control, and HeLa cell extract served as the positive control. A similar analysis was performed using all other samples (data not shown). Right panel, Densitometry analysis of total STAT3 and serine p-STAT3 of cells from patients with CLL with low ($n = 32$) and high ($n = 32$) lymphocyte counts normalized to the β -actin level is depicted. As shown, total STAT3 levels were higher in cells from patients with high lymphocyte counts, whereas serine p-STAT3 levels were not significantly different in patients with high and low lymphocyte counts. **(B)** STAT3 levels of CLL cells from 64 patients with CLL, quantified using densitometry analysis of Western immunoblotting analysis, were plotted against the patients' WBC counts. Spearman test was used to calculate the correlation between STAT3 and the patients' WBC counts. **(C)** Western immunoblot analysis of CLL cells from patients with low ($n = 9$; median WBC = 20.8; range 3.3–35.7 $\times 10^9/L$) and high ($n = 6$; median WBC = 107.2; range 56.7–130 $\times 10^9/L$) lymphocyte counts using STAT1 and p-STAT1 Abs. HeLa and NIH323 cell lines were used as positive controls. The medians of densitometry levels were compared using the Mann-Whitney U test. As shown, unphosphorylated STAT1 and serine p-STAT1 levels were similar in cells from patients with high and low lymphocyte counts. Tyrosine p-STAT1 was not detected.

with the caspase-3 DNA promoter fragment, and the binding was completely reversed by the addition of excess unlabeled probe (Fig. 6A). Unlike the isotype control IgG, anti-serine p-STAT3 Abs attenuated the binding, and no binding was detected when a

biotinylated mutated site 1 DNA probe was used instead of the site 1 probe. In addition, using ChIP, we found that CLL cell chromatin fragments that were immunoprecipitated with anti-STAT3 Abs coimmunoprecipitated with DNA of caspase-3 and

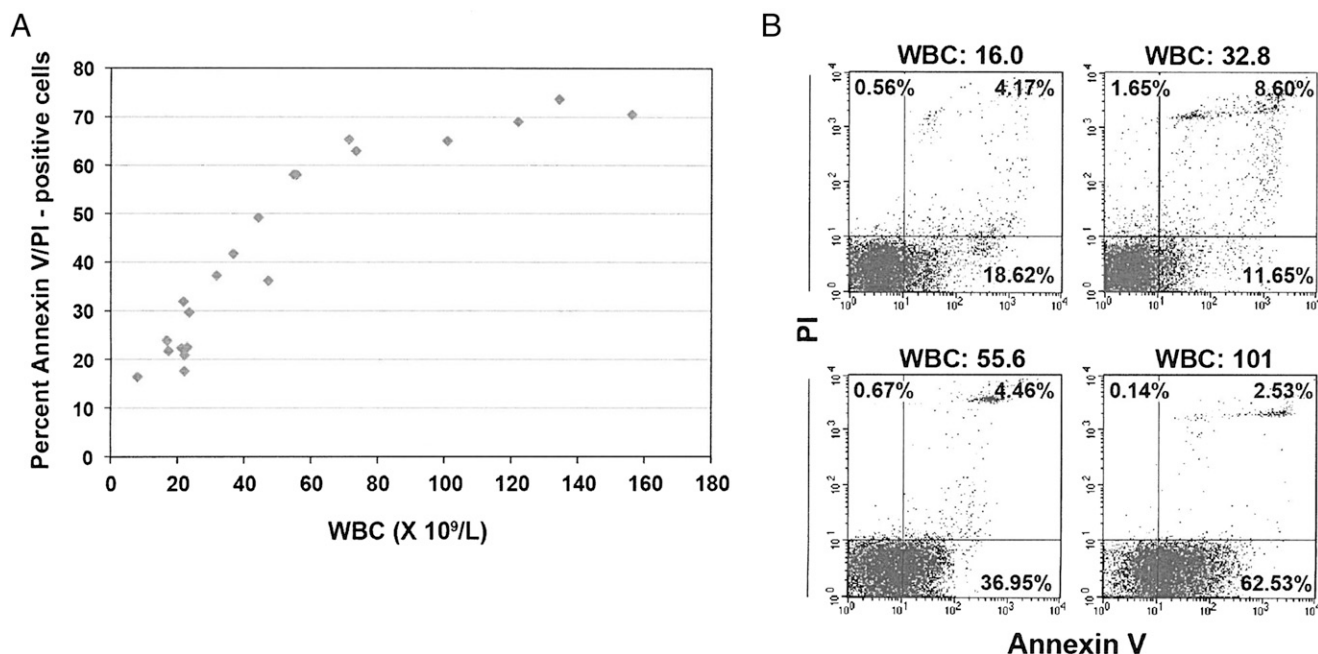


FIGURE 2. Peripheral lymphocytes of patients with CLL undergo spontaneous apoptosis. **(A)** Spontaneous apoptosis rates of freshly obtained low-density cells from 19 patients with CLL. Cellular apoptosis was assessed using flow cytometry following Annexin V/PI staining. Rates of spontaneous apoptosis correlated with WBC counts ($r_p = 0.88$; $p < 0.0001$ **(A)**. **(B)** Shown are rates of spontaneous apoptosis (early, lower right quadrant; late, upper right quadrant) of four patients with low, intermediate, and high WBC counts.

the STAT3-regulated genes STAT3, p21, c-Myc, retinoic acid-related orphan receptor 1, and vascular endothelial growth factor-C (Fig. 6B). Taken together, these data suggest that STAT3 binds to the *caspase-3* promoter.

Like in other cancers, in CLL, STAT3 provides the neoplastic cells with a survival advantage (10). However, overexpression of STAT3 induced a significant increase in caspase-3 expression and induced apoptotic cell death. Furthermore, CLL cells from patients with a high, but not low, lymphocyte count expressed high levels of STAT3 and underwent spontaneous apoptosis at a high rate. Therefore, using Western immunoblotting, we assessed the levels of caspase-3 in CLL cells from patients with high and low lymphocyte counts and found that caspase-3 and cleaved caspase-3 levels were significantly higher in cells from patients with high counts (Fig. 6C). We then plotted the levels of caspase-3

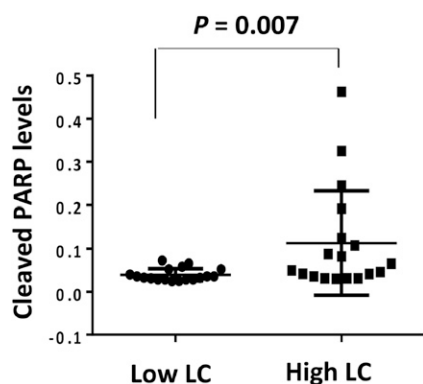


FIGURE 3. Cleaved PARP levels are high in CLL cells from patients with high lymphocyte counts (LC). CLL cell ($ng/5 \times 10^5$ cells) cleaved PARP levels were measured by ELISA using PB cells from 32 patients. Median cleaved PARP levels in cells of patients with low ($n = 16$) and high ($n = 16$) lymphocyte counts were analyzed using the Mann-Whitney U test. As shown, the levels of cleaved PARP were significantly higher in cells from patients with high lymphocyte counts ($p < 0.007$).

as a function of the levels of total STAT3 and found that caspase-3 remained constant across a wide range of STAT3 levels and increased only when a threshold of STAT3 protein level was reached (Fig. 6D), suggesting that the binding affinity of p-STAT3 to the *caspase-3* promoter is relatively weak and that p-STAT3 activates the transcription of caspase-3 only when its levels are sufficiently high.

To test this hypothesis, we first used ChIP. Serial dilutions of CLL cell DNA of chromatin fragments coimmunoprecipitated with anti-STAT3 Abs were prepared, and STAT3 target genes were detected via PCR. As opposed to p21, c-Myc, or STAT3, caspase-3 was detected only in the least diluted fraction, suggesting that STAT3 binds to the *caspase-3* promoter with a low affinity (Fig. 6E). We also analyzed the DNA that coimmunoprecipitated with STAT3 by using qRT-PCR. High c-Myc, p21, and STAT3 but low caspase-3 levels were detected. As in MM-1 cells, DNA of the *Caspase-3* promoter was detected using primer sets 1, 2, and 4 but not with primer set 3 (Fig. 6F). These results confirmed that STAT3 binds to the *caspase-3* promoter with low affinity.

To further delineate these findings, we performed EMSA. Using serial dilutions of CLL cell nuclear extracts, we found that the binding of those extracts to the biotinylated *caspase-3* promoter DNA probe was low compared with the binding of *c-Myc* or *STAT3* promoter probes across all tested dilutions (Fig. 6G). Furthermore, the binding of nuclear extracts of CLL cells from patients with low lymphocyte counts ($n = 4$) was significantly lower than that of patients with high counts ($n = 4$) (Fig. 6H), suggesting that nuclear extracts from patients with CLL with high lymphocyte counts bind to the *caspase-3* promoter with a higher affinity.

Discussion

In this study, we show that when present at high levels, p-STAT3 activates caspase-3 and induces apoptosis. For decades, the relatively slow accumulation of CLL cells in most patients was attributed to a prolonged lifespan of the leukemia cells (2–4, 28). However, evidence from recent years suggests that CLL cells proliferate and die, cell birth and death rates are similar, and

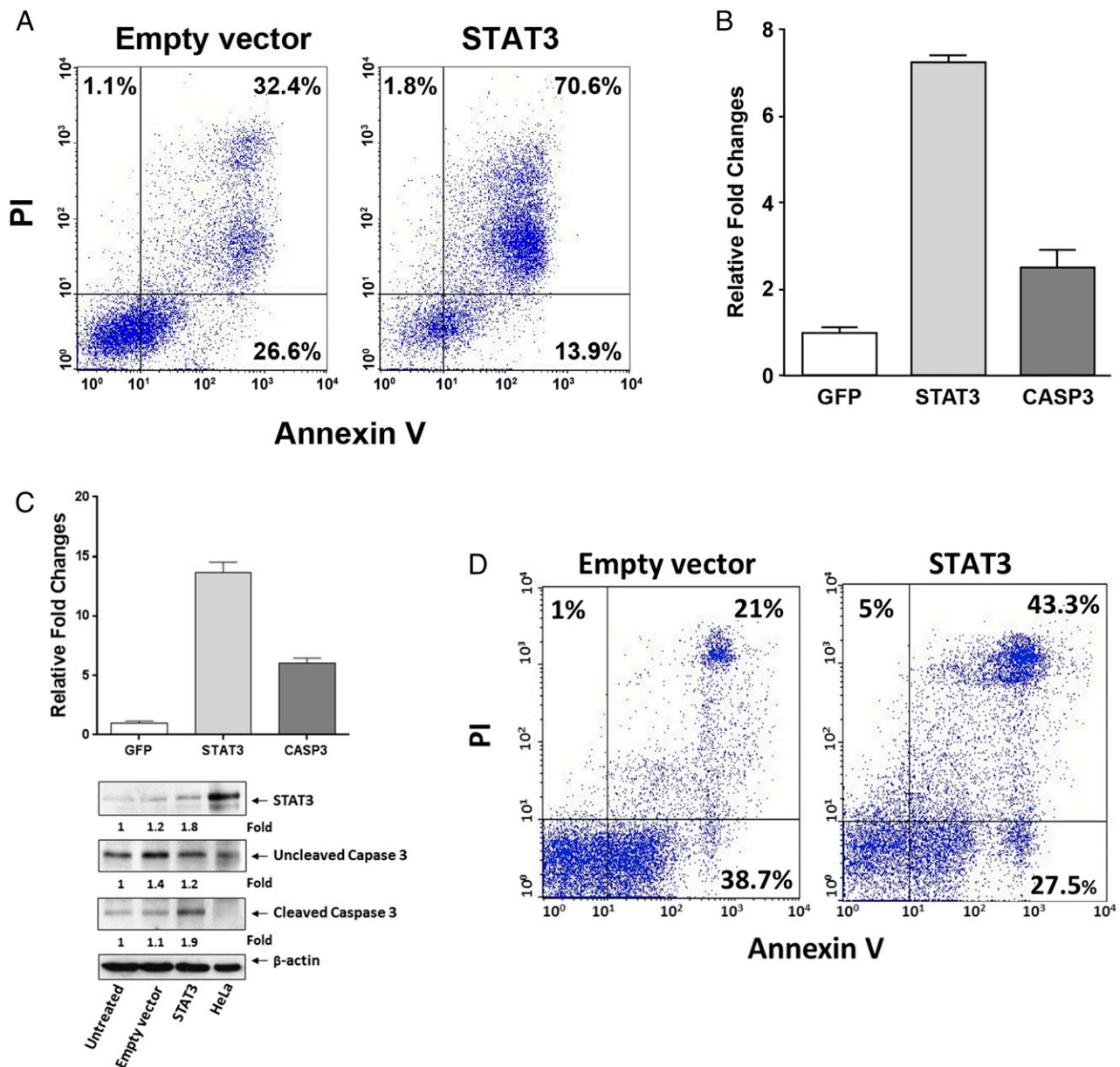


FIGURE 4. Overexpression of STAT3 upregulates caspase-3 and induces apoptosis in MM-1 and CLL cells. **(A)** MM-1 cells were transfected via electroporation with a mammalian vector that coexpressed the full-length STAT3 sequence and GFP or with the same vector expressing only GFP (empty vector) and stimulated with IL-6. Using double staining for Annexin V/PI, we detected the cellular apoptosis rate via flow cytometry 24 h after the transfection. As shown, at a transfection rate of 42%, 85% of CLL cells transfected with STAT3 underwent apoptosis compared with a 59% apoptosis rate of cells transfected with the empty vector. A representative figure from three different experiments is depicted. In all experiments, apoptosis rate was higher in MM-1 cell transfected with rSTAT3 DNA ($p < 0.001$; paired t test). **(B)** Relative expression of STAT3 and caspase-3 mRNA assessed via qRT-PCR in MM-1 cells transfected with STAT3 and stimulated with IL-6. Compared to control untransfected cells, STAT3 and caspase-3 RNA levels were markedly upregulated. RNA levels of STAT3 and caspase-3 in STAT3-transfected MM-1 cells. As shown, transfection of MM-1 cells with STAT3 induced a 7.5-fold increase in STAT3 and a 2.5-fold increase in caspase-3 RNA levels. The means \pm SD of gene expression fold change from three different experiments are depicted. **(C)** *Top panel*, Relative expression of STAT3 and caspase-3 mRNA assessed using qRT-PCR in CLL cells infected with a lentivirus harboring the human STAT3 gene. CLL cells were infected with the full-length STAT3 gene sequence. As shown, overexpression of STAT3 ($\geq 30\%$ infection efficiency) induced a 13.5-fold increase in STAT3 and a 6-fold increase in caspase-3 RNA levels. The means \pm SD of gene expression fold change from three different experiments using the same patient's cells are depicted. *Bottom panel*, Protein levels of STAT3 and uncleaved and cleaved caspase-3 of the same patient's cells assessed by Western immunoblotting and quantitated by densitometry. As shown, STAT3 levels increased by 0.6-fold and cleaved caspase-3 levels by 0.8-fold compared with their corresponding levels in cells infected with the empty vector. Similar results were obtained using CLL cells from two other patients with low lymphocyte counts. **(D)** Apoptosis rate of the CLL cells infected with the full-length STAT3 gene or the empty vector assessed by flow cytometry 24 h postinfection. As shown, at an infection rate of 30%, the apoptosis rate of CLL cells transfected with STAT3 was 70.8%, whereas that of cells infected with the empty vector was 59.7%. Similar results were obtained using cells from two other patients with low lymphocyte counts.

the actual CLL cell count represents a net effect of clonal turnover (24).

Like in several cancers, in CLL, STAT3 is constitutively activated (8, 11, 17, 19, 29, 30). Activated STAT3 functions as an

oncogene that induces proliferation and protects the neoplastic cells from apoptosis (10, 14, 31, 32). STAT3 activates the STAT3 gene, and as a result, CLL cells harbor high levels of STAT3 (10). As anticipated, STAT3 levels correlated with the patients' lymphocyte

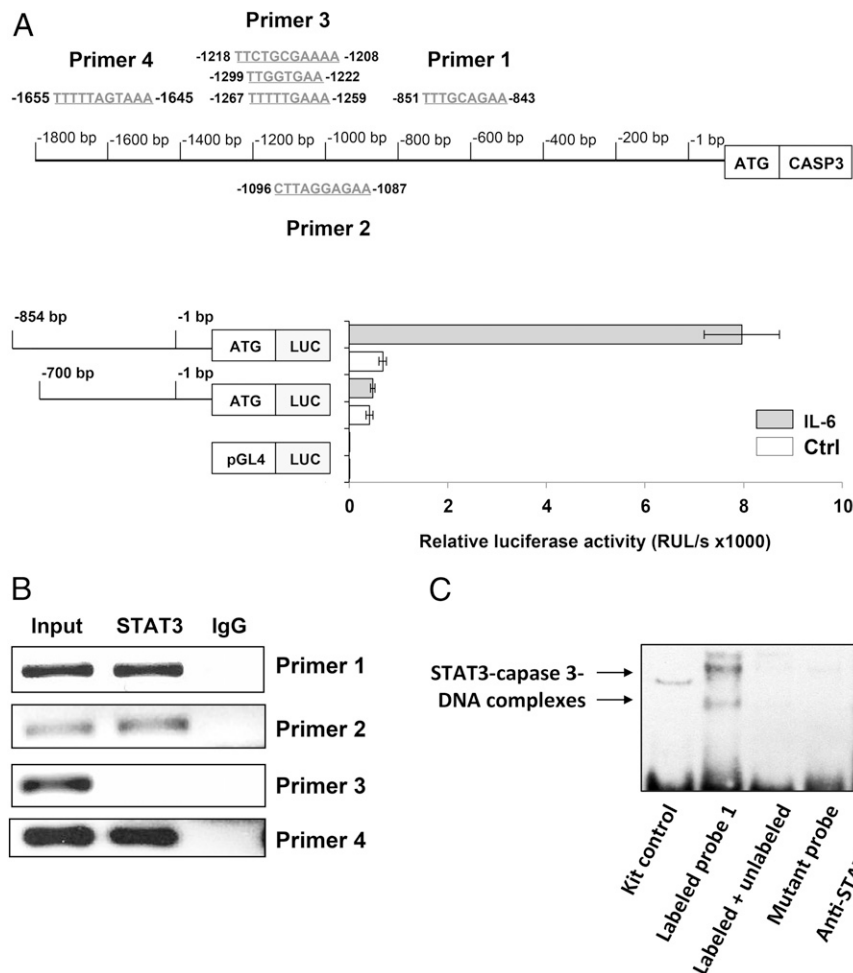


FIGURE 5. STAT3 binds to and activates the caspase-3 gene promoter in MM-1 cells. **(A)** *Top panel*, Schematic diagram of the 1.8-kb DNA sequence located at the 5' transcription starting site of the caspase-3 gene promoter. In this region, we identified six GAS-like elements. Primers 1–4 were designed to capture these putative STAT3 binding sites. *Bottom panel*, MM-1 cells were transfected with a reporter construct that included the luciferase gene and either the 770 bp that did not include a GAS-like element or the 854-bp sequence that included a single GAS-like element flanking the 5' region of the caspase-3 gene. After incubation with IL-6, which induces the phosphorylation of STAT3, luciferase activity was detected only in cells transfected with the longer caspase-3 promoter construct that included STAT3 binding sites. The means \pm SD of four different experiments are depicted. **(B)** MM-1 cell were incubated for 30 min with 30 ng/ml IL-6, and DNA was extracted prior to (input) or after ChIP with anti-STAT3 Abs. As shown, DNA from the *caspase-3* promoter was detected via PCR with primers 1, 2, and 4, but not primer 3, corresponding to the STAT3 putative binding sites 1–4. **(C)** MM-1 cell nuclear extract was incubated with a biotinylated DNA probe that included a putative STAT3 binding site detected via ChIP with primer set 1 in the *caspase-3* promoter. EMSA showed that the CLL cell nuclear extract bound the biotinylated DNA probe, excess unlabeled probe reversed the binding, anti-STAT3 Abs (but not IgG) attenuated the binding, and there was no binding to the biotinylated mutated DNA probe, suggesting that CLL cell nuclear STAT3 bound the caspase-3 promoter. Representative data from three duplicate experiments that yielded identical results are depicted. Ctrl, control.

count. However, in patients with high counts, STAT3 induced apoptosis rather than providing the cells with a survival advantage. This functional switch occurred only in cells with significantly high STAT3 levels. Likewise, overexpression of STAT3 induced apoptosis in MM-1 cells and in CLL cells from patients with relatively low lymphocyte counts.

In various neoplasms, STAT1 and STAT3 undergo similar post-translation modifications (33). Consistent with our data, in CLL, both STAT1 and STAT3 are constitutively phosphorylated on serine 727 residues (10, 22) but not on tyrosine residues (34–36). However, whereas activated STAT3 under most conditions protects the cells from apoptosis (10, 12, 13, 22), activated STAT1 induces apoptosis (37). Remarkably, unlike STAT3, STAT1 or serine p-STAT1 levels did not correlated with CLL patients' lymphocyte counts, suggesting that the proapoptotic effect of STAT3 is independent of STAT1.

Theoretically, at high levels, STAT3 might promote apoptosis either directly or indirectly by no longer activating antiapoptotic genes. In a previous study, we found that in acute myeloid leukemia,

GM-CSF, known to induce myeloid cell proliferation, also upregulated and activated proapoptotic caspases by activating the JAK–STAT signaling pathway (38). The results of that study suggested that STAT activation induces apoptosis by directly activating the apoptotic cell death machinery. In the current study, we found that the transcript levels of the STAT3-regulated antiapoptotic genes Bcl-2 and MCL-1 were similar in CLL cells from patients with high and low lymphocyte counts, suggesting that these antiapoptotic genes are not downregulated in cells from patients with high lymphocyte counts. However, in cells from patients with high lymphocyte counts, caspase-3 levels were significantly high, suggesting that when present at high levels, STAT3 activates caspase-3.

In mammalian cells, STAT3 is ubiquitously expressed as a latent isoform and is activated upon phosphorylation on tyrosine 705 residues (39). In circulating CLL cells, STAT3 is constitutively phosphorylated on serine but not tyrosine residues (10, 22), and both serine- and tyrosine-p-STAT3 activate a similar repertoire of genes (12, 13, 19, 36). By using a luciferase assay of IL-6-stimulated

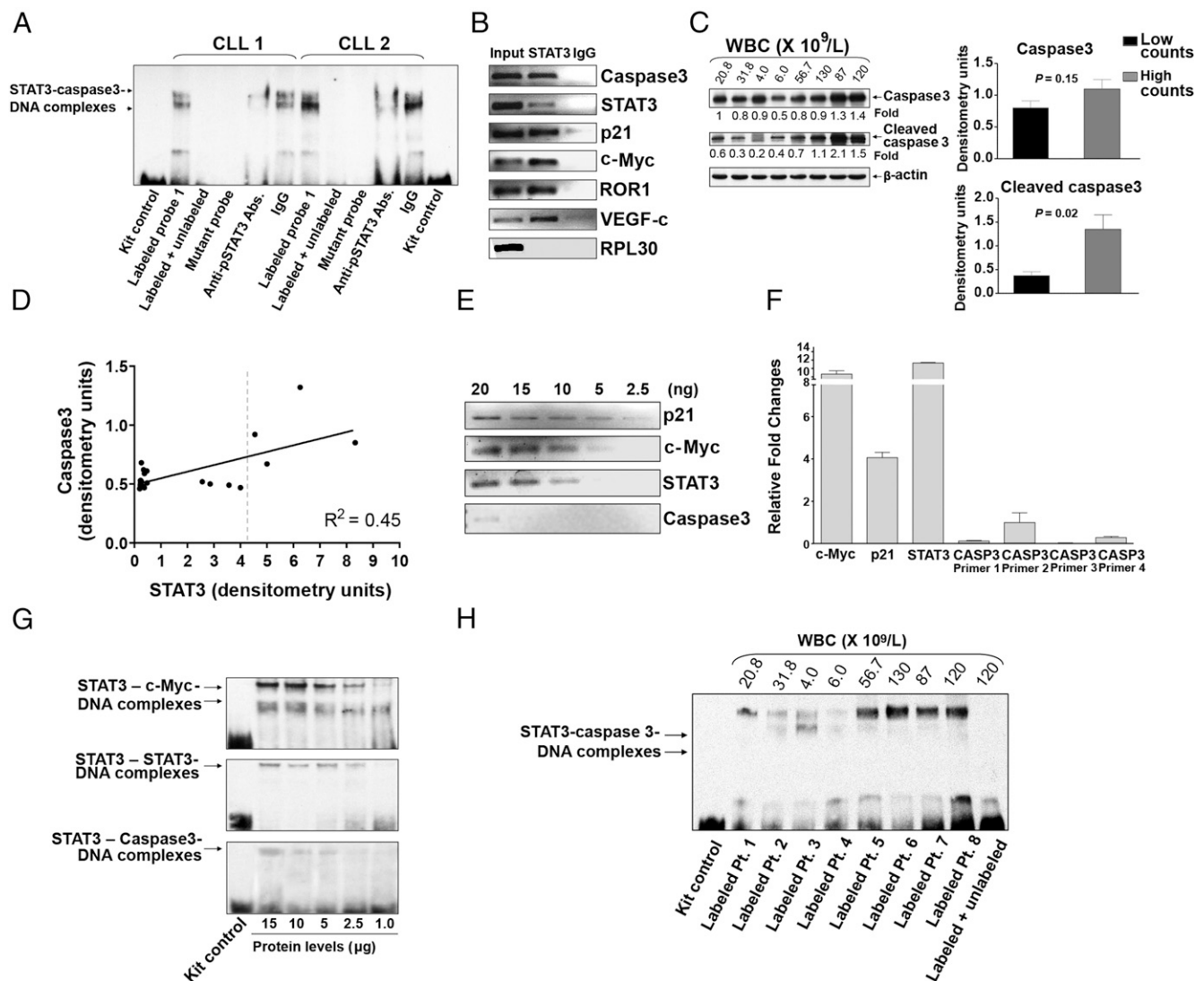


FIGURE 6. STAT3 binds with low affinity to the caspase-3 gene promoter in CLL cells. **(A)** Nuclear extracts of CLL cells from two patients with high lymphocyte counts were incubated with biotinylated probe that included the putative STAT3 binding site detected by primer 1. EMSA showed that the protein extracts from both patients bound the caspase-3 DNA probe. The addition of excess unlabeled probe reversed the binding, anti-serine pSTAT3 Abs (but not IgG) attenuated the binding, and there was no binding to the biotinylated mutated DNA probe. **(B)** ChIP of CLL cells. CLL cell chromatin fragments were immunoprecipitated with anti-STAT3 Abs, the coimmunoprecipitated DNA was isolated, and STAT3 target genes were detected via PCR. As shown, the DNA of caspase-3, STAT3, p21, c-Myc, retinoic acid-related orphan receptor 1 (ROR1), and vascular endothelial growth factor (VEGF)-C coimmunoprecipitated with STAT3. RPL30 promoter was used as a negative control. This experiment was repeated four times using samples from four different patients. Similar results were obtained in all experiments. **(C) Left panel,** Western immunoblot analysis of CLL cells from patients with low ($n = 4$) and high ($n = 4$) lymphocyte counts. The membrane depicted in Fig. 1B was reprobed using caspase-3 and cleaved caspase-3 Abs. **Right panel,** Densitometry analysis of the Western blot data shown in the left panel. **(D)** STAT3 and caspase-3 levels were assessed simultaneously in CLL cells from 24 patients via Western blot analysis and quantitated using densitometry, by which the level obtained in every lane was normalized to the levels of actin. The figure depicts a correlation between the levels of STAT3 and caspase-3. As shown, the levels of caspase-3 remained constant across a wide range of STAT3 levels and linearly increased with increasing STAT3 levels behind a threshold (vertical dotted line). A linear regression model (black line) that fits 45% of the variance ($R^2 = 0.45$) is depicted. **(E)** CLL cell chromatin fragments were immunoprecipitated with anti-STAT3 Abs. Serial dilutions of the DNA (2.5–20 ng) that were coimmunoprecipitated with STAT3 were prepared, and STAT3-regulated genes were detected via PCR. As shown, caspase-3 was detected only in the least diluted (20 ng) DNA preparation. In contrast, p21, c-Myc, and STAT3 were also detected in the 5 ng (p21 and c-Myc) and 10 ng (STAT3) dilutions. This experiment was repeated four times. **(F)** The binding affinity of four putative STAT3 binding sites in the caspase-3 promoter of CLL cells was compared with that of *c-Myc*, *p21*, and *STAT3* using qRT-PCR. As in MM-1 cells, *caspase-3* was detected by primers 1, 2, and 4 but not by primer 3, and the relative fold change in *c-Myc*, *p21*, and *STAT3* gene expression was significantly higher than that of caspase-3, indicating that the binding affinity of STAT3 to *c-Myc*, *p21*, and *STAT3* promoters is stronger than the binding affinity of STAT3 to the caspase-3 promoter. The data depicted are from three separate experiments. **(G)** EMSA comparing the binding of serial dilutions (1–15 μ g) of CLL cell nuclear protein to biotinylated promoter probes of the STAT3-regulated genes *c-Myc*, *STAT3*, and *caspase-3*. As shown, only a high concentration (15 μ g) of nuclear protein bound to the caspase-3 promoter probe, whereas lower concentrations of nuclear protein bound *c-Myc* or *STAT3* biotinylated promoter probes. Similar data were generated using a sample from another patient. **(H)** EMSA of CLL cell nuclear extracts from patients with high and low lymphocyte counts. A labeled *caspase-3* promoter probe was used. As shown, DNA binding of STAT3 to the *caspase-3* promoter probe was significantly lower in nuclear extracts from patients with low (median: $13.3 \times 10^9/l$; range 4–31.8) versus high (median: $103 \times 10^9/l$; range 56.7–130) WBC counts. The addition of an unlabeled probe (right lane) attenuated the binding of STAT3 to the *caspase-3*-labeled probe.

MM-1 cells, in which IL-6 induces tyrosine-p-STAT3 (25), we found that p-STAT3 activates the *caspase-3* promoter. These data were confirmed by ChIP and an EMSA with Abs that detect phosphorylated and unphosphorylated STAT3 isoforms. In CLL cells, ChIP confirmed that STAT3 binds with low affinity to the *caspase-3* promoter, and an EMSA revealed that specific anti-serine p-STAT3 Abs significantly attenuated the binding of pSTAT3 to the *caspase-3* promoter, suggesting that serine-p-STAT3 rather than its unphosphorylated form activates the *caspase-3* promoter in CLL cells.

Caspase-3 levels increased only when STAT3 levels reached a threshold. High levels of STAT3 were required to induce this effect because the binding affinity of p-STAT3 to the caspase-3 gene promoter is relatively low. Hence, the functional switch of STAT3 depends on its DNA-binding affinity. However, DNA-binding affinity cannot be predicted by a consensus sequence per se. STAT3-DNA binding may vary depending on background DNA sequences in the vicinity to the GAS element, the chromatin status, and concomitant binding of STAT or DNA structures to other proteins, adaptor molecules, and other factors (40). For example, we identified several GAS-like elements in the *caspase-3* promoter and used primers to detect them. However, one primer (primer 3), constructed to detect a STAT3-specific (TTCN3GAA) binding element, did not detect STAT3-caspase-3-DNA binding in MM-1 or CLL cells. Although analyzing STAT3 binding sites in the genome of different species, we did not detect conserved sequence blocks within the *caspase-3* promoter. However, we identified several putative STAT3 binding sites in the *caspase-3* promoter of all examined organisms.

STAT3 binds with high affinity to the antiapoptotic Bcl-2 and MCL-1 gene promoters and with low affinity to the caspase-3 gene promoter, suggesting that in CLL cells from patients with high lymphocyte counts, the activation of the caspase-3 gene overcomes in part the protective effect of antiapoptotic genes, and apoptotic cell death ensues.

Caspase-3 is an inactive zymogen that is usually activated by the intrinsic and the extrinsic apoptotic pathways (41). By activating the caspase-3 gene, STAT3 increases the level of caspase-3 and predisposes it to proteolytic cleavage by upstream caspases such as caspase-8 or caspase-9. In CLL cells, STAT3 levels correlated with the levels of cleaved but not uncleaved caspase-3 possibly because as its levels increased, caspase-3 underwent rapid cleavage. Unlike other caspases that possess autocatalytic activity, an intrinsic safety catch prevents the autocatalysis of caspase-3. Upon removal of the safety catch by acidification or other means, caspase-3 undergoes autocatalytic cleavage (42). Whether autocatalysis or upstream caspases activate caspase-3 in CLL cells remains to be determined.

Whereas in normal cells extracellular stimuli activate STAT3, in CLL, STAT3 is constitutively phosphorylated and activated. p-STAT3 forms dimers, shuttles to the nucleus using the karyopherin nuclear transport system, binds to DNA, and, following nuclear phosphatase-induced dephosphorylation, STAT3 translocates to the cytosol using nuclear export chromosome region maintenance 1 (10). In the nucleus, p-STAT3 binds primarily to high-affinity DNA-binding sites, and when present at excess, p-STAT3 dimers bind to low-affinity DNA-binding sites. In the cytosol, a cytoplasmic serine kinase phosphorylates the USTAT3 on serine 727 residues (Z. Estrov, unpublished observations); in addition, USTAT3 binds to the NF- κ B in competition with I κ B (19). The levels of serine p-STAT3 detected via Western immunoblotting were similar in CLL cells of patients with high or low lymphocyte counts, most likely because this assay is not suitable to detect miniscule, albeit biologically significant, changes in p-STAT3 levels. Given that p-STAT3 activates the STAT3 gene and induces the production of STAT3 protein (10), cellular levels of total STAT3 protein represent a

better parameter of the activity of STAT3. Therefore, it is very likely that in CLL cells from patients with high lymphocyte counts, both USTAT3 and p-STAT3 levels are high.

USTAT3 activates NF- κ B (19), and, like the NFAT, NF- κ B is constitutively activated in unstimulated CLL cells. Together, these transcription factors orchestrate a transcription program that further protects CLL cells from apoptosis (19, 43–45). Like STAT3, NF- κ B levels correlate with disease burden (46), and although generally viewed as an antiapoptotic transcription factor, NF- κ B also harbors proapoptotic properties (47).

Excessive activation of STAT3 induces apoptosis of CLL cells. Whether this versatile effect represents a physiological negative-feedback mechanism used in normal cells to counteract extreme proliferation or unwarranted prolonged cellular survival remains to be determined.

Acknowledgments

We thank Markeda Wade of the Department of Scientific Publications at The University of Texas MD Anderson Cancer Center for editing the manuscript.

Disclosures

The authors have no financial conflicts of interest.

References

- Chiorazzi, N., K. R. Rai, and M. Ferrarini. 2005. Chronic lymphocytic leukemia. *N. Engl. J. Med.* 352: 804–815.
- Bentley, D. P., and C. J. Pepper. 2000. The apoptotic pathway: a target for therapy in chronic lymphocytic leukemia. *Hematol. Oncol.* 18: 87–98.
- Dameshek, W. 1967. Chronic lymphocytic leukemia—an accumulative disease of immunologically incompetent lymphocytes. *Blood* 29(4, Suppl):566–584.
- Kitada, S., I. M. Pedersen, A. D. Schimmer, and J. C. Reed. 2002. Dysregulation of apoptosis genes in hematopoietic malignancies. *Oncogene* 21: 3459–3474.
- Bueso-Ramos, C. E., A. Ferrajoli, L. J. Medeiros, M. J. Keating, and Z. Estrov. 2004. Aberrant morphology, proliferation, and apoptosis of B-cell chronic lymphocytic leukemia cells. *Hematology* 9: 279–286.
- Chiorazzi, N. 2007. Cell proliferation and death: forgotten features of chronic lymphocytic leukemia B cells. *Best Pract. Res. Clin. Haematol.* 20: 399–413.
- Wang, X., P. J. Crowe, D. Goldstein, and J. L. Yang. 2012. STAT3 inhibition, a novel approach to enhancing targeted therapy in human cancers (review). *Int. J. Oncol.* 41: 1181–1191.
- Alvarez, J. V., H. Greulich, W. R. Sellers, M. Meyerson, and D. A. Frank. 2006. Signal transducer and activator of transcription 3 is required for the oncogenic effects of non-small-cell lung cancer-associated mutations of the epidermal growth factor receptor. *Cancer Res.* 66: 3162–3168.
- Garcia, R., T. L. Bowman, G. Niu, H. Yu, S. Minton, C. A. Muro-Cacho, C. E. Cox, R. Falcone, R. Fairclough, S. Parsons, et al. 2001. Constitutive activation of Stat3 by the Src and JAK tyrosine kinases participates in growth regulation of human breast carcinoma cells. *Oncogene* 20: 2499–2513.
- Hazan-Halevy, I., D. Harris, Z. Liu, J. Liu, P. Li, X. Chen, S. Shanker, A. Ferrajoli, M. J. Keating, and Z. Estrov. 2010. STAT3 is constitutively phosphorylated on serine 727 residues, binds DNA, and activates transcription in CLL cells. *Blood* 115: 2852–2863.
- Kusaba, T., T. Nakayama, K. Yamazumi, Y. Yakata, A. Yoshizaki, K. Inoue, T. Nagayasu, and I. Sekine. 2006. Activation of STAT3 is a marker of poor prognosis in human colorectal cancer. *Oncol. Rep.* 15: 1445–1451.
- Li, P., S. Grgurevic, Z. Liu, D. Harris, U. Rozovski, G. A. Calin, M. J. Keating, and Z. Estrov. 2013. Signal transducer and activator of transcription-3 induces microRNA-155 expression in chronic lymphocytic leukemia. *PLoS One* 8: e64678.
- Li, P., D. Harris, Z. Liu, J. Liu, M. Keating, and Z. Estrov. 2010. Stat3 activates the receptor tyrosine kinase like orphan receptor-1 gene in chronic lymphocytic leukemia cells. *PLoS One* 5: e11859.
- Liu, Y., P. K. Li, C. Li, and J. Lin. 2010. Inhibition of STAT3 signaling blocks the anti-apoptotic activity of IL-6 in human liver cancer cells. *J. Biol. Chem.* 285: 27429–27439.
- Malyukova, A., T. Dohda, N. von der Lehr, S. Akhoondi, M. Corcoran, M. Heyman, C. Spruck, D. Grandér, U. Lendahl, and O. Sangfelt. 2007. The tumor suppressor gene hCDC4 is frequently mutated in human T-cell acute lymphoblastic leukemia with functional consequences for Notch signaling. *Cancer Res.* 67: 5611–5616.
- Morikawa, T., Y. Baba, M. Yamauchi, A. Kuchiba, K. Noshio, K. Shima, N. Tanaka, C. Huttenhower, D. A. Frank, C. S. Fuchs, and S. Ogino. 2011. STAT3 expression, molecular features, inflammation patterns, and prognosis in a database of 724 colorectal cancers. *Clin. Cancer Res.* 17: 1452–1462.

17. Yin, W., S. Cheepala, J. N. Roberts, K. Syson-Chan, J. DiGiovanni, and J. L. Clifford. 2006. Active Stat3 is required for survival of human squamous cell carcinoma cells in serum-free conditions. *Mol. Cancer* 5: 15.
18. Ferrajoli, A., S. Faderl, Q. Van, P. Koch, D. Harris, Z. Liu, I. Hazan-Halevy, Y. Wang, H. M. Kantarjian, W. Priebe, and Z. Estrov. 2007. WP1066 disrupts Janus kinase-2 and induces caspase-dependent apoptosis in acute myelogenous leukemia cells. *Cancer Res.* 67: 11291–11299.
19. Liu, Z., I. Hazan-Halevy, D. M. Harris, P. Li, A. Ferrajoli, S. Faderl, M. J. Keating, and Z. Estrov. 2011. STAT-3 activates NF-kappaB in chronic lymphocytic leukemia cells. *Mol. Cancer Res.* 9: 507–515.
20. Bromberg, J. F., M. H. Wrzeszczynska, G. Devgan, Y. Zhao, R. G. Pestell, C. Albanese, and J. E. Darnell, Jr. 1999. Stat3 as an oncogene. *Cell* 98: 295–303.
21. Sansone, P., and J. Bromberg. 2012. Targeting the interleukin-6/Jak/stat pathway in human malignancies. *J. Clin. Oncol.* 30: 1005–1014.
22. Frank, D. A., S. Mahajan, and J. Ritz. 1997. B lymphocytes from patients with chronic lymphocytic leukemia contain signal transducer and activator of transcription (STAT) 1 and STAT3 constitutively phosphorylated on serine residues. *J. Clin. Invest.* 100: 3140–3148.
23. Avallé, L., S. Pensa, G. Regis, F. Novelli, and V. Poli. 2012. STAT1 and STAT3 in tumorigenesis: A matter of balance. *JAK-STAT* 1: 65–72.
24. Chiorazzi, N., and M. Ferrarini. 2006. Evolving view of the in-vivo kinetics of chronic lymphocytic leukemia B cells. *Hematology (Am Soc Hematol Educ Program)* 273–278, 512.
25. Amit-Vazina, M., S. Shishodia, D. Harris, Q. Van, M. Wang, D. Weber, R. Alexanian, M. Talpaz, B. B. Aggarwal, and Z. Estrov. 2005. Atiprimod blocks STAT3 phosphorylation and induces apoptosis in multiple myeloma cells. *Br. J. Cancer* 93: 70–80.
26. Berishaj, M., S. P. Gao, S. Ahmed, K. Leslie, H. Al-Ahmadie, W. L. Gerald, W. Bornmann, and J. F. Bromberg. 2007. Stat3 is tyrosine-phosphorylated through the interleukin-6/glycoprotein 130/Janus kinase pathway in breast cancer. *Breast Cancer Res.* 9: R32.
27. Leu, C. M., F. H. Wong, C. Chang, S. F. Huang, and C. P. Hu. 2003. Interleukin-6 acts as an antiapoptotic factor in human esophageal carcinoma cells through the activation of both STAT3 and mitogen-activated protein kinase pathways. *Oncogene* 22: 7809–7818.
28. Robertson, L. E., W. Plunkett, K. McConnell, M. J. Keating, and T. J. McDonnell. 1996. Bcl-2 expression in chronic lymphocytic leukemia and its correlation with the induction of apoptosis and clinical outcome. *Leukemia* 10: 456–459.
29. Chung, S. S., C. Aroh, and J. V. Vadgama. 2013. Constitutive activation of STAT3 signaling regulates hTERT and promotes stem cell-like traits in human breast cancer cells. *PLoS One* 8: e83971.
30. Garner, J. M., M. Fan, C. H. Yang, Z. Du, M. Sims, A. M. Davidoff, and L. M. Pfeffer. 2013. Constitutive activation of signal transducer and activator of transcription 3 (STAT3) and nuclear factor κ B signaling in glioblastoma cancer stem cells regulates the Notch pathway. *J. Biol. Chem.* 288: 26167–26176.
31. Glienke, W., E. Hausmann, and L. Bergmann. 2011. Downregulation of STAT3 signaling induces apoptosis but also promotes anti-apoptotic gene expression in human pancreatic cancer cell lines. *Tumour Biol.* 32: 493–500.
32. Uckun, F., Z. Ozer, and A. Vassilev. 2007. Bruton's tyrosine kinase prevents activation of the anti-apoptotic transcription factor STAT3 and promotes apoptosis in neoplastic B-cells and B-cell precursors exposed to oxidative stress. *Br. J. Haematol.* 136: 574–589.
33. Regis, G., S. Pensa, D. Boselli, F. Novelli, and V. Poli. 2008. Ups and downs: the STAT1:STAT3 seesaw of Interferon and gp130 receptor signalling. *Semin. Cell Dev. Biol.* 19: 351–359.
34. Battle, T. E., and D. A. Frank. 2003. STAT1 mediates differentiation of chronic lymphocytic leukemia cells in response to Bryostat 1. *Blood* 102: 3016–3024.
35. Battle, T. E., W. G. Wierda, L. Z. Rassenti, D. Zahrie, D. Neuberg, T. J. Kipps, and D. A. Frank. 2003. In vivo activation of signal transducer and activator of transcription 1 after CD154 gene therapy for chronic lymphocytic leukemia is associated with clinical and immunologic response. *Clin. Cancer Res.* 9: 2166–2172.
36. Rozovski, U., J. Y. Wu, D. M. Harris, Z. Liu, P. Li, I. Hazan-Halevy, A. Ferrajoli, J. A. Burger, S. O'Brien, N. Jain, et al. 2014. Stimulation of the B-cell receptor activates the JAK2/STAT3 signaling pathway in chronic lymphocytic leukemia cells. *Blood* 123: 3797–3802.
37. Liang, X., E. A. Moseman, M. A. Farrar, V. Bachanova, D. J. Weisdorf, B. R. Blazar, and W. Chen. 2010. Toll-like receptor 9 signaling by CpG-B oligodeoxynucleotides induces an apoptotic pathway in human chronic lymphocytic leukemia B cells. *Blood* 115: 5041–5052.
38. Faderl, S., D. Harris, Q. Van, H. M. Kantarjian, M. Talpaz, and Z. Estrov. 2003. Granulocyte-macrophage colony-stimulating factor (GM-CSF) induces anti-apoptotic and proapoptotic signals in acute myeloid leukemia. *Blood* 102: 630–637.
39. Darnell, J. E., Jr. 1997. STATs and gene regulation. *Science* 277: 1630–1635.
40. Ehret, G. B., P. Reichenbach, U. Schindler, C. M. Horvath, S. Fritz, M. Nabholz, and P. Bucher. 2001. DNA binding specificity of different STAT proteins. Comparison of in vitro specificity with natural target sites. *J. Biol. Chem.* 276: 6675–6688.
41. Liu, H., D. W. Chang, and X. Yang. 2005. Interdimer processing and linearity of procaspase-3 activation. A unifying mechanism for the activation of initiator and effector caspases. *J. Biol. Chem.* 280: 11578–11582.
42. Roy, S., C. I. Bayly, Y. Gareau, V. M. Houtzager, S. Kargman, S. L. Keen, K. Rowland, I. M. Seiden, N. A. Thornberry, and D. W. Nicholson. 2001. Maintenance of caspase-3 proenzyme dormancy by an intrinsic "safety catch" regulatory tripeptide. *Proc. Natl. Acad. Sci. USA* 98: 6132–6137.
43. Chandra-Kuntal, K., and S. V. Singh. 2010. Diallyl trisulfide inhibits activation of signal transducer and activator of transcription 3 in prostate cancer cells in culture and in vivo. *Cancer Prev. Res. (Phila.)* 3: 1473–1483.
44. Lee, E. S., K. K. Ko, Y. A. Joe, S. G. Kang, and Y. K. Hong. 2011. Inhibition of STAT3 reverses drug resistance acquired in temozolomide-resistant human glioma cells. *Oncol. Lett.* 2: 115–121.
45. Real, P. J., A. Sierra, A. De Juan, J. C. Segovia, J. M. Lopez-Vega, and J. L. Fernandez-Luna. 2002. Resistance to chemotherapy via Stat3-dependent overexpression of Bcl-2 in metastatic breast cancer cells. *Oncogene* 21: 7611–7618.
46. Hewamana, S., S. Alghazal, T. T. Lin, M. Clement, C. Jenkins, M. L. Guzman, C. T. Jordan, S. Neelakantan, P. A. Crooks, A. K. Burnett, et al. 2008. The NF-kappaB subunit Rel A is associated with in vitro survival and clinical disease progression in chronic lymphocytic leukemia and represents a promising therapeutic target. *Blood* 111: 4681–4689.
47. Radhakrishnan, S. K., and S. Kamalakaran. 2006. Pro-apoptotic role of NF-kappaB: implications for cancer therapy. *Biochim. Biophys. Acta* 1766: 53–62.